SAND2008-2894C

HEAT FLUX FROM AMBIENT AIR SOLID PROPELLANT FIRE PLUMES

Walt Gill[1], Bill Erikson[2], Vern Nicolette[1], and John Hewson[1]
[1]Fire and Aerosol Sciences
[2]Nanoscale and Reactive Processes
Sandia National Laboratories
Albuquerque, NM 87185

ABSTRACT

Radiant heat flux data from ambient air solid propellant fire plumes to nearby objects have been gathered from firings performed under well-controlled conditions. Cylinders of aluminized composite solid propellant were inhibited to restrict burning to a single planar face and placed in a 6 m cube-like enclosure that allowed total control and measurement of the ambient conditions. The cylinders were oriented with the burning surface facing upward. Propellant cylinders with diameters ranging from 6 in (152 mm) to 20 in (508 mm) were observed with heat flux sensors placed at multiple locations with respect to the burning surface. The resulting heat flux readings are compared to results from high fidelity computational simulations. Agreement and differences are discussed with implications on the understanding of these propellant fire plumes.

INTRODUCTION

Open-air solid propellant fires represent a broad class of possible launch system accident scenarios that must be understood and analyzed in order to evaluate system safety. In these hypothetical scenarios the rocket motor cases have been breached and large pieces of solid propellant are scattered and burned at atmospheric pressure. Objects of interest are then exposed to burning rocket propellant plumes either indirectly by being in the proximity or directly by being engulfed in the plume flow.

A significant effort is underway to develop a first-principles based multi-physics computational simulation capability to capture solid fuel propellant fire phenomena for launch system safety studies. Validation quality data is needed for these models in the region of application. Validation quality requires well controlled experiments with well defined boundary conditions that often need to be iterated with computational predictions. This places limitations on the availability of suitable archival data, and thus requires new experimentation.

To meet this need, radiant heat flux data from ambient air solid propellant fire plumes to near-by objects have been gathered from firings performed under well controlled conditions. Cylinders of aluminized composite solid propellant configured to burn in cigarette mode (end-burning) with the plume in an upward direction were placed in a 6 m cube like enclosure that allowed total control and measurement of the ambient conditions. Propellant cylinder diameters ranged from 6 in (152 mm) to 20 in (508 mm). Observations were made with heat flux sensors placed at multiple locations with respect to the burning surface. Air flow rates and temperatures into and out of the enclosure were monitored as well.

In what follows, the experiments are first described and some results are shown. Then the multiphysics computational fire code VULCAN propellant fire model is presented in light of the experimental heat flux readings. Agreement and differences for both models and the data are then discussed with implications on the understanding of these propellant fire plumes.

EXPERIMENT

FIRE FACILITY

FLAME (Fire Laboratory for Accreditation of Modeling by Experiment) is an enclosed hydrocarbon pool fire test facility located at the Lurance Canyon Burn Facility at Sandia National Laboratories. It was designed to meet air quality regulations in tests conducted with hydrocarbon fuels. However, it is exceptionally well suited for conducting midscale propellant fires as well. The original FLAME contained a 2-meter diameter pool in a 6-meter cubed test chamber fitted with water cooled walls. The pan is located on an elevated pedestal while inlet air enters in a ring at floor level. This arrangement is amenable to modeling, allows close control of thermal and flow boundary conditions, and is of a size of interest for propellant fire model validation exercises (Fig.1).

In the present experiments, a cylindrical sample of AP/HTPB/Al composite propellant is placed on the center of the elevated pedestal with diagnostics located in the surrounding areas. The propellant sample is side inhibited so as to burn in a planar fashion, beginning at the upper flat surface and regressing down towards the pedestal surface. Instrumentation was located though out the facility, and notably for this paper, a tower fitted with heat flux gauges was placed off to one side. (Fig. 2) The nominal locations given in inches correspond to the height above the initial propellant surface. A table in the figure gives the locations with respect to the center of the pedestal surface (x and z being the horizontal and vertical coordinates respectively). The initial propellant burning surface is centered at x= 0, z = 0.1016 m.

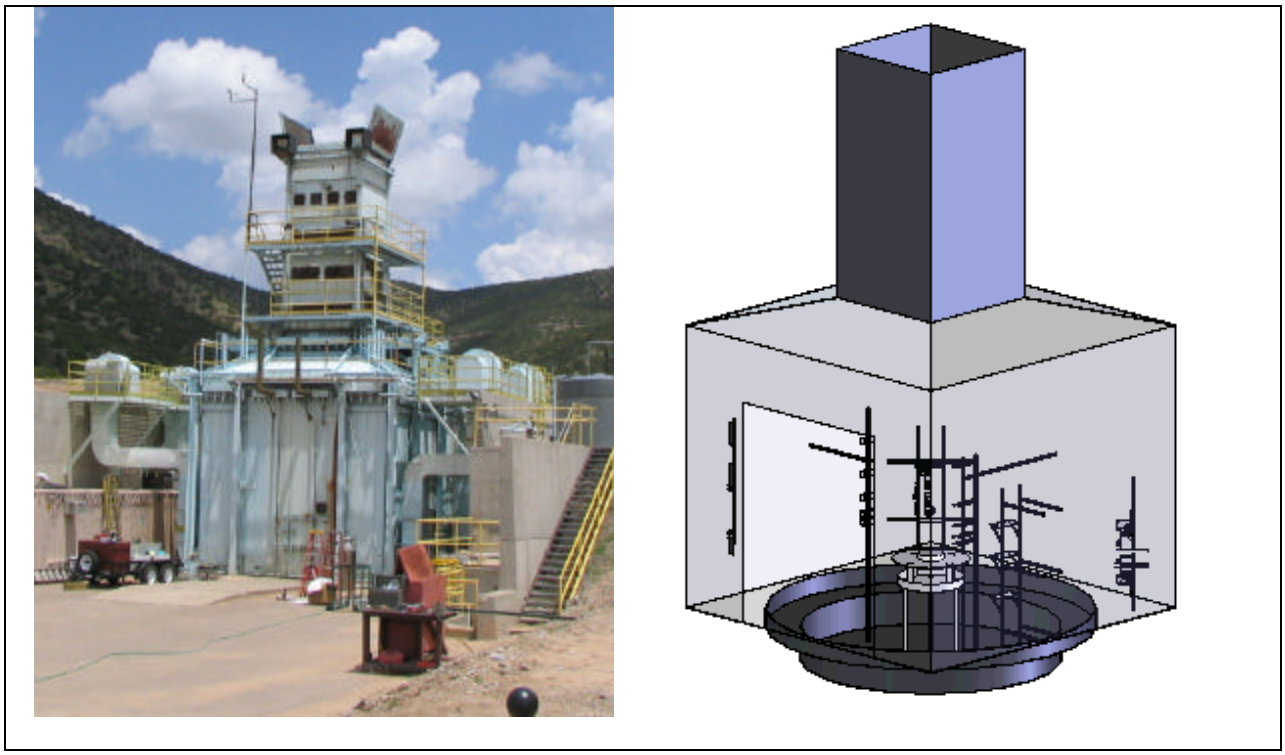

Figure 1. FLAME fire facility photo and cutaway view of internal features

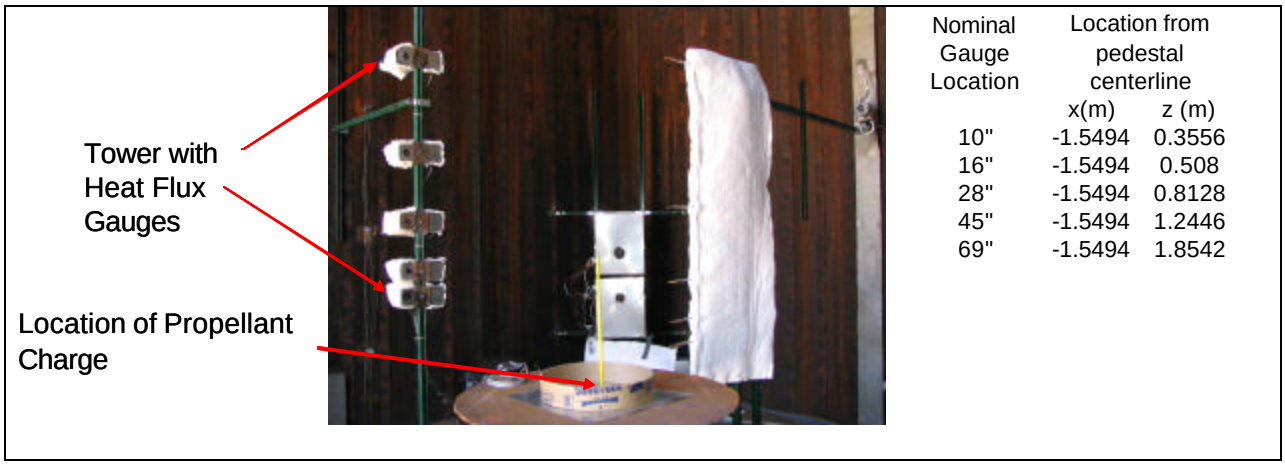

Nominal Gauge Location	Location from pedestal centerline x(m)	z (m)
10"	-1.5494	0.3556
16"	-1.5494	0.508
28"	-1.5494	0.8128
45"	-1.5494	1.2446
69"	-1.5494	1.8542

Figure 2. Internal view of setup with locations of heat flux gauges. The cardboard ring represents the size and location of a 20 inch diameter propellant charge. Other instrumentation is evident.

DESCRIPTION OF HEAT FLUX GAUGE

The heat flux is measured by exposing one side of a thin metal plate to the fire environment and observing the temperature response. Ideally, the plate is perfectly isolated, i.e., the unexposed side and the edges of the plate are thermally insulated. Furthermore, if the plate is assumed to be thermally thin, gradients through the plate and along the lateral direction can be ignored. These assumptions allow interpreting the temperature measured at a single point on the unexposed surface as the one-dimensional response of a heated composite wall.

To meet the requirements of a one-dimensional response, the Sandia Heat Flux Gauge (HFG) shown in Figure 2 was developed [1]. The assembly is essentially a hollow cylinder filled with thermal insulation that is fitted with sensor plates on each end. The body of the HFG is a 10-cm long cylinder of 10.2-cm diameter schedule 40 steel pipe. The body is filled with Cerablanket® ceramic fiber insulation to minimize heat transfer inside the HFG. The entire assembly is held together with four stainless steel bolts. The sensor plates are 10.2-cm squares of 0.025-cm thick 304 stainless steel shim-stock. The plates are held in place on the cylindrical body by endplates that are 10.2-cm square by 0.32-cm thick 304 stainless steel with a centered 5.0-cm hole. The sensor surfaces are thermally isolated from the remainder of the HFG by two layers of Lytherm® ceramic fiber insulation. The front sides of the sensor surfaces are coated with Pyromark® paint to achieve a diffuse gray surface. A 0.16-cm diameter Inconel-sheathed type-K thermocouple is used as the sensor thermocouple. The sensor thermo couple is attached to the sensor surface with 0.01-cm thick retainer straps that are spot-welded to the back of the sensor surface. For the data taken here, the gauge has been constructed with only one sensor plate. Only one end was exposed to the fire, and the sensor plate on the other end was replaced with a flat plate.

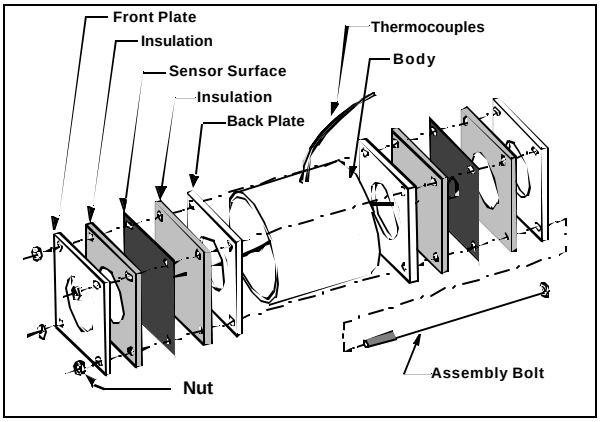

Figure 3. The Sandia HFG.

The recorded time-temperature history is processed via software specifically developed for this gauge. The output of the software includes the incident heat flux and the uncertainty as a function of time. Uncertainty sources for the gauge include uncontrolled variability, missing physics, and simplifying assumptions in the use of the gauge. They amount to a total uncertainty in heat flux on the order of 20%.

EXPERIMENTS AND RESULTS

Four separate experiments were conducted, each with a different propellant sample diameter. The diameters were a nominal 20", 18", 12" and 6" with each being a nominal 4" thick. They were in inhibited on the side so as to burn from one face only with the plume oriented upward. Ignition was obtained from an electric match and propellant crumbles on the surface (Fig. 4).

Figure 4. A 20" dia propellant sample with cardboard side inhibitor. The ignition charge is propellant crumbles and an electric match.

Fig 5 shows the resultant heat flux received by the gauges on the tower as a function of time for the 20" charge. As can be seen in the figure the propellant burned for ~100 seconds. This data was time average for the middle 80 seconds and analyzed for uncertainty. The results for all 4 tests are shown in Fig 6. In that figure, the uncertainty of the measurement is indicated by error bars which are approximately 20% of the reading. The obvious trends of lower fluxes with smaller propellant diameter are expected. The rise and fall in heat flux levels with height are perhaps not so expected, however, the trends are within the stated uncertainty limits, and as such may not be significant.

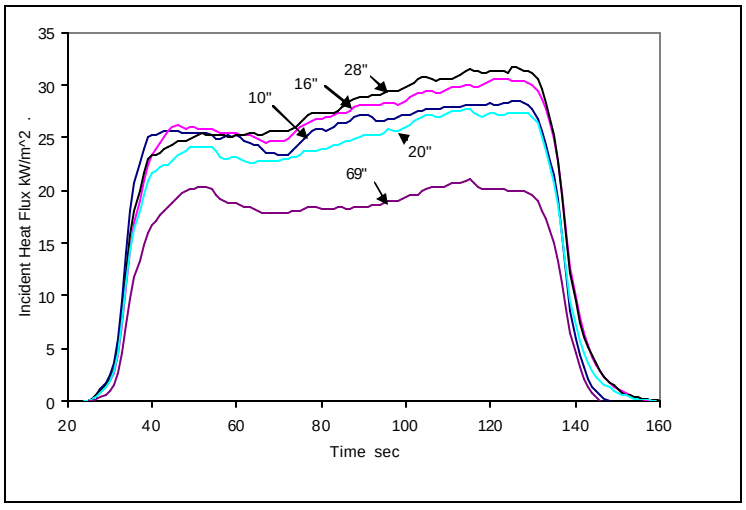

Figure 5. Heat flux vs. time for the 20" dia charge. The heat flux gauge nominal locations are noted on the plot.

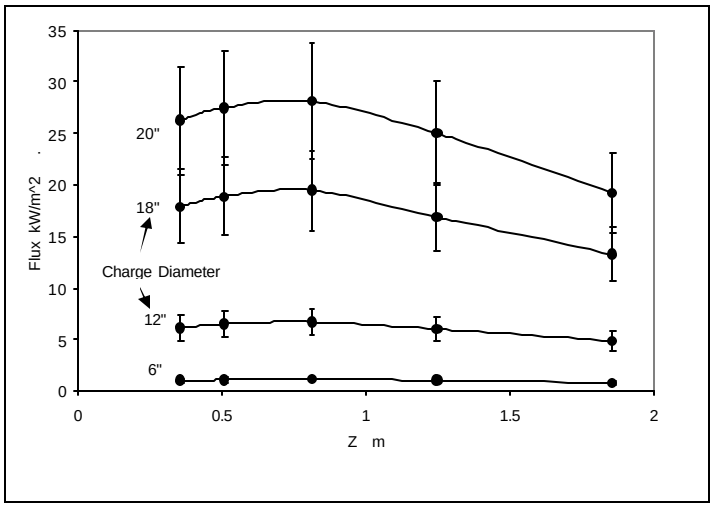

Figure 6. Heat flux as function of location on the tower and propellant charge diameter.

MODEL

VULCAN FIRE MODEL

The Vulcan fire model is a first-principles computational fluid dynamics (CFD) fire model originally developed for simulating hydrocarbon pool and jet fires, which has recently been extended to model ambient atmosphere solid propellant fires [2]. The extensions included propellant fire chemistry and aluminum droplet burning.

Thermal radiation to/from the aluminum droplet, the diffusion flame/comet, and the agglomerated alumina smoke is included in the model. The alumina smoke is treated as a heavy gas, and transported on the Eulerian grid as a pseudo-gas species. Optical properties of alumina are taken from Parry and Brewster [3]. The aluminum droplets are treated in a Lagrangian manner, and parcels of droplets are injected into the flow and tracked with time. The sub-oxide diffusion flame is treated with a subgrid model, and provides a source/sink term to the local control volume species and energy equations, as well as the radiation transport equation. Vulcan calculates gas temperatures, but does not specifically calculate diffusion flame temperatures around the droplets. Instead, the diffusion flame energy released is deposited into the local gas control volumes. Hence, there is no radiation directly from the diffusion flames ('halos' or 'comets'), but rather from the bulk gas and alumina and aluminum in a given control volume.

The droplet model is capable of handling distributions of droplet velocities, diameters and temperatures. Aerodynamic interactions between the droplets and the surrounding gas phase are modeled, as are droplet impacts with surfaces. Droplet trajectories are determined by the droplet diameter, initial velocity, acceleration, and interactions with other droplets and the surrounding gas phase (see Hewson et al. [4]). The droplets heat up and cool down based on local convective and radiative heat transfer with the surroundings. A model is implemented for evaporation of the droplets (which causes the droplet diameter to decrease), and combustion of the aluminum vapor that results. The combustion process can occur with 3 different oxidizers (O_2, H_2O, and CO_2).

The Vulcan model has submodels for the gas radiation from CO_2 and H_2O. For solid propellants, the species HCl is also an important contributor to the gas radiation. The model of Fuss and Hamins [5] was used for the HCl species, so that HCl could be included with the other gas emitters. All gas radiation is spectral in nature, and hence the absorption/emission coefficients are functions of wavelength. Since the current model uses a gray gas assumption, a Planck mean absorption coefficient is computed for each participating gas species mentioned above by weighting the spectral absorption coefficients by the emissive power at that wavelength, integrating over all wavelengths, and then dividing by the integral of the emissive power over all wavelengths. This method will not account for saturation of individual gas bands.

Thermal radiation from the particles and from the gases is modeled using the Discrete Transfer Method (DTM) of Shah [6]. The DTM model is based on a ray tracing approach, and is often utilized in CFD fire models because of its

robustness and ability to model irregular geometries. Thermal radiation from surfaces, gases and particles is treated by the model. Once the local temperature and emissivity of each control volume are calculated, the intensity of thermal radiation is solved for by sending out and tracking rays of intensity through each control volume. The gradient in intensity across a control volume is used to determine the divergence of the radiation heat flux vector in each control volume, which is part of the gas energy equation. While the DTM method is general enough to handle scattering as well as emission/absorption, we have only utilized it for the emission/absorption in the present work. Additionally, the gaseous, particle, and surface radiation are considered to be 'gray', i.e., independent of wavelength in the present work.

20" DIAMETER CHARGE RESULTS

The Vulcan model results are shown in the table below. Simulations were conducted with a nominal base case, and with variations (+ and -) on the alumina smoke emissivity and the aluminum droplet emissivity. The alumina smoke emissivity was increased by an order of magnitude and also decreased by an order of magnitude to account for uncertainties in the data due to impurities, different measurement techniques, and measurement uncertainty. The aluminum droplet emissivity was increased by a factor of 5 and also decreased by a factor of 5 to reflect uncertainties in the precise value due to alumina formation and measurement uncertainty. The nominal case represents an alumina smoke emissivity representative of pure alumina as function of volume fraction and temperature [3], so we would expect the case with an order of magnitude increase in alumina smoke emissivity to perhaps be more representative of the general case where impurities are present. The nominal case also represents an aluminum droplet emissivity of 0.1, representative of pure aluminum. We would expect the case with a factor of 5 increase in droplet emissivity to be more representative of the general case where alumina is also present on the droplet surface.

Table 1 Vulcan model radiative heat flux results for 20" case

Tower Location	Nominal (kW/m^2)	Smoke / 10 (kW/m^2)	Smoke * 10 (kW/m^2)	Droplet / 5 (kW/m^2)	Droplet * 5 (kW/m^2)
10"	35.9	31.7	49.8	36.2	35.1
16"	31.6	26.8	49.7	32.0	31.2
28"	28.4	25.8	35.1	28.6	27.0
45"	31.7	28.5	39.8	31.9	30.8
69"	29.6	26.8	34.0	29.8	28.9

All of the simulation results were obtained over a 1 – 2 second burn duration following aluminum particle injection, and have been time averaged once the initial transient fluctuations were removed (i.e., only the quasi-steady portion of the results was time averaged). The Vulcan results vary significantly with the alumina smoke emissivity, but not so much with the aluminum droplet emissivity. These model results are substantially higher than the data for all of the cases simulated (38 – 56%), and span the range of 26 – 50 kW/m^2.

Trends can be compared between the experiment and model as shown in Fig 7. The experimental results show a weak indication of a peak heat flux at the nominal 28" location. However, the experimental results are close enough to one another that they could reasonably be regarded as having the same value of heat flux at all these elevations.

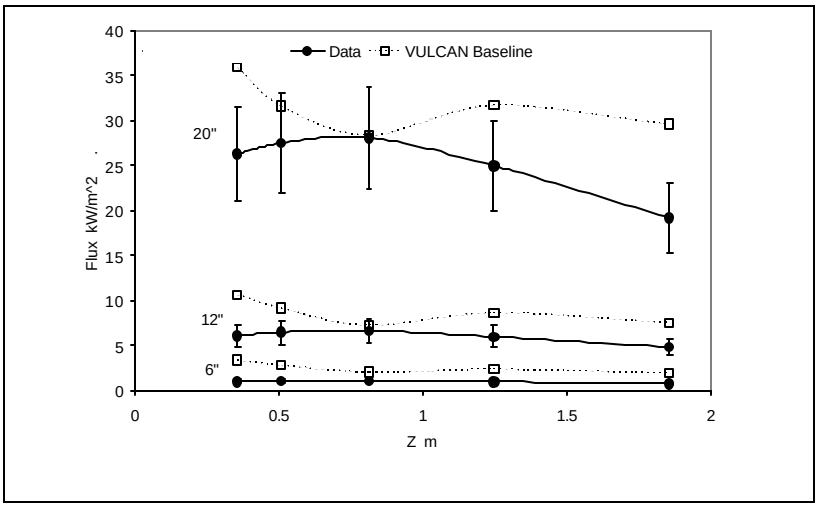

Figure 7. Comparison of measured heat flux with values obtained from VULCAN. The VULCAN values are for the baseline case.

The variation in modeling results from elevation to elevation shows a different trend with height. The heat fluxes at higher elevations are significantly lower than that at the 10" elevation, with the exception of the simulation with the alumina smoke emissivity increased by an order of magnitude. For that case, the value of heat flux at 16" was within 0.1 W/m^2 of that at 10". The modeling results also indicate that the 28" elevation represents the lowest heat flux for all but the case with the alumina smoke emissivity increased by an order of magnitude, in contrast to the experimental results. To understand the model trends, it is instructive to consider the model results for the heat flux contributors (plume temperature and overall emissivity, and alumina mass fraction). The model results predict the highest plume temperatures to be relatively low in elevation, and decreasing with height (apart from a few inches near the charge surface where the aluminum ignition process is occurring, and hence temperatures increase with height over the first few inches above the charge surface). See Fig 8a for illustration. This could explain why the highest heat flux observed in the model results is located near the lowest elevation.

The model also predicts a gradually increasing plume emissivity with elevation (Fig 8b). Note that Fig 8a is a time average of the model results, whereas the remaining figures with model results are instantaneous snapshots in time. The plume absorption coefficient is relatively constant with elevation until the alumina in the plume reaches a temperature below about 2300 K, at which point the absorption coefficient starts to significantly increase (see Fig 9a). Over the first roughly 1 m elevation, the alumina mass fraction in the plume increases everywhere (Fig 9b) due to the production of alumina from aluminum. Above this elevation the mass fraction of alumina does not substantially change, indicating most of the aluminum has burned out. The increase in plume absorption coefficient at elevations where the temperature has dropped below 2300 K is due primarily to the increased absorption efficiency of alumina smoke for temperatures below 2300 K. The increased absorption efficiency of alumina smoke is caused by the phase transition of the smoke from liquid to solid alumina.

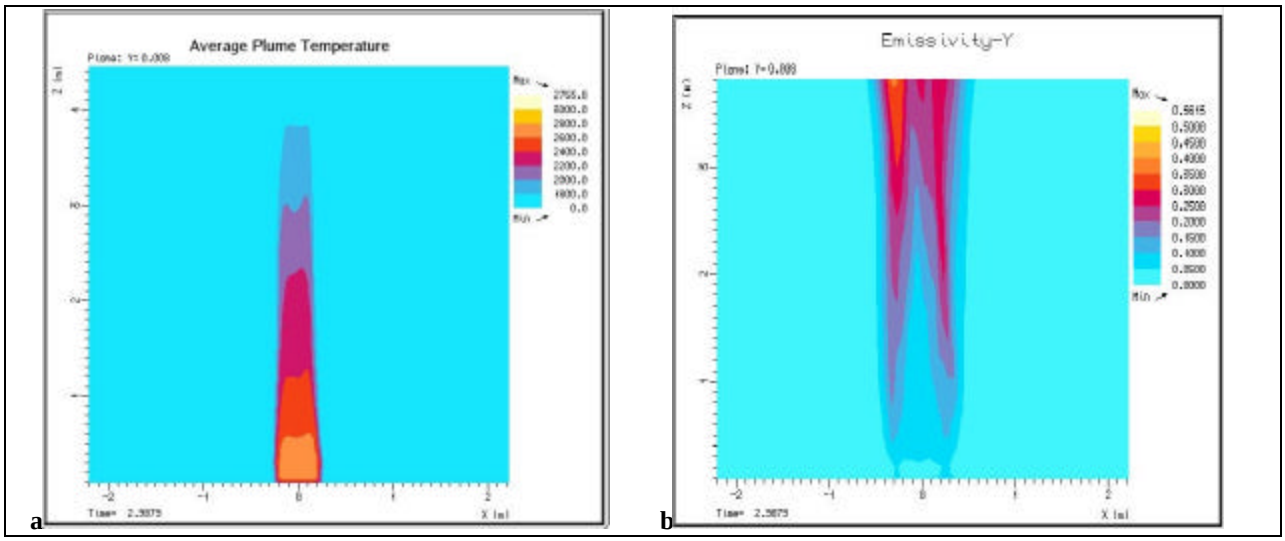

Figure 8. Model results for time-averaged plume temperature and instantaneous plume emissivity (vertical slice through plume) Emissivity is the integration of the absorption coefficient multiplied by the path length along each line of sight.

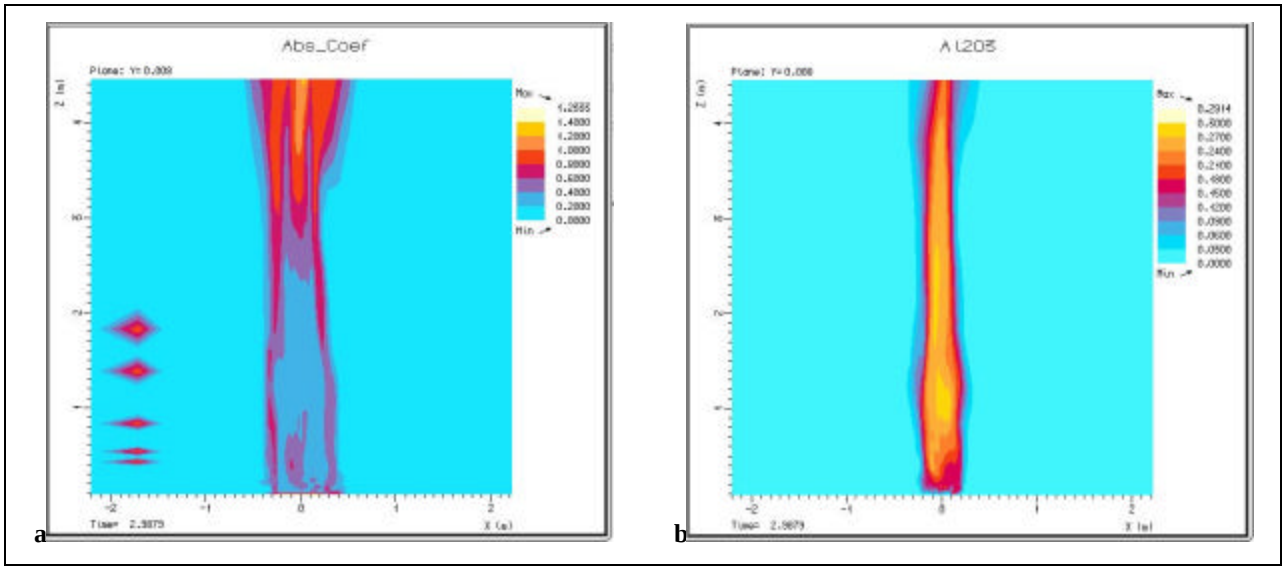

Figure 9. Model results for instantaneous absorption coefficient (inverse meters) and alumina mass fraction shown along a vertical slice through plume. The 5 blips to the left are the tower heat flux gauge locations. Note: The cooler alumina along the edge of the plume has a higher absorption coefficient because of the increased absorption efficiency of alumina at temperatures below the melting point (~ 2300 K).

The model results that generally indicate the lowest heat flux to be at the middle measurement location (28") represent a location where the decreasing plume temperature (with elevation) has not been offset enough by the increasing emissivity to avoid yielding a minimum.

12" and 6" DIAMETER CHARGE RESULTS

Heat fluxes are substantially lower for this smaller charge case, and range from 5 – 8 kW/m^2. Once again the highest elevation measures the lowest heat flux. For the other elevations, there is not much difference in the value of

heat flux. The Vulcan modeling results are shown in Table 2 below for the 12" and 6"charge cases, with nominal conditions only.

Table 2 Vulcan model radiative heat flux results for 12"and 6" charge cases

Tower Location	12" Nominal (kW/m^2)	6" Nominal (kW/m^2)
10"	10.7	3.4
16"	9.2	2.9
28"	7.3	2.1
45"	8.7	2.4
69"	7.6	2.0

The modeling results for heat flux for the 12" diameter nominal case range from 7.3 – 10.7 kW/m^2. This is substantially higher (34 – 50%) than the measured values of 5 – 8 kW/m^2. The modeling results for the 6" diameter nominal case range from 2.0 – 3.4 kW/m^2. Again, the modeling result is higher than the measured values of 1 – 2 kW/m^2.

The 12" case was run two more times with different input conditions. For both of these cases the particle initial temperature was set to 1800 K (previous simulations set the initial particle temperature equal to the initial gas temperature just above the charge surface). The initial gas temperature was increased to 2257 K to conserve energy, consistent with the results of the thermo-equilibrium code (Propep GDL). Additionally, for the second of these two cases, the radiation from the charge surface was set to be consistent with that of a blackbody at 1000 K (previous results assumed that the charge surface was a blackbody at the initial gas temperature just above the charge surface). The results are shown in Table 3.

Table 3 Vulcan model radiative heat flux results for 12"case: different inputs

Tower Location	12" with Tp=1800 K (kW/m^2)	12" with Tp=1800 K and charge surface at 1000 K (kW/m^2)
10"	10.6	7.3
16"	8.7	7.9
28"	7.1	6.7
45"	8.5	7.8
69"	7.3	7.0

The modeling results for heat flux for the 12" diameter case with Tp=1800 K and the charge surface represented by a blackbody at the gas temperature range from 7.1 – 10.6 kW/m^2. This is again significantly higher than the measured values of 5 – 8 kW/m^2. Changing the initial particle temperature to 1800 K (from a value of about 2190 K in the previous 12" simulation) has little effect on the results. The modeling results for heat flux for the 12" diameter case with Tp=1800 K and the charge surface represented by a blackbody at 1000 K range from 6.7 – 7.9 kW/m^2. This is within the range of measured values of 5 – 8 kW/m^2.

A plot of the values Table 3 compares the results with the data (Fig 10.). It can be seen that the modeled propellant surface temperature is of importance. The plume is optically thin and the heat flux gauges can radiatively 'see' the charge surface. It has been recognized that the burning surface was an important boundary condition for objects in the plume but not suspected that temperature and emissivity of the charge surface would be important contributors to the resultant heat fluxes to objects at a distance as well.

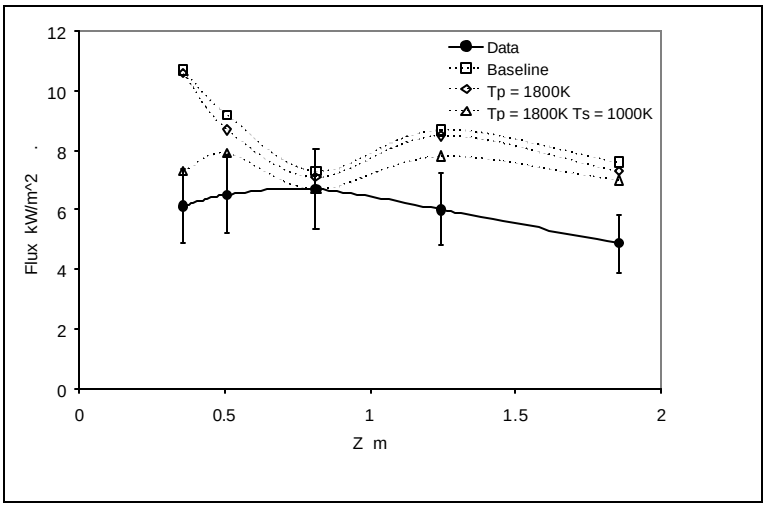

Figure 10. Comparisons of data from the 12" dia case with simulation results for different modeling parameters.

CONCLUSIONS

The Vulcan model has been compared to experimental measurements for heat flux at a distance from burning charges of solid rocket propellant. Assuming that the charge surface can be represented by a blackbody at the initial gas temperature, the model appears to be conservative in that it generally over-predicts the data by 35 – 55 % for all charge sizes. When the charge surface is assumed to be a blackbody at 1000 K, and the initial particle temperature is assumed to be 1800 K, the model predictions for heat flux are within the range of the measured data. Since the plume is optically thin, the assumptions on the temperature and emissivity of the charge surface appear to have the most influence on the results. Model trends for heat flux can be understood in terms of the detailed modeling results for plume temperature, absorption coefficient, emissivity, and alumina mass fraction.

ACKNOWLEDGMENTS

This work was supported by DOE Campaign 6 and was performed at Sandia National Laboratories, a multi-program laboratory operated by Sandia Corporation, a Lockheed-Martin Company, for the United States Department of Energy under Contract DE-AC04-94AL85000.

REFERENCES

1. Blanchat, T.K., and Humphries, L.L., Gill, W., 'Sandia Heat Flux Gauge Thermal Response and Uncertainty Models ," *Thermal Measurements: The Foundation of Fire Standards, ASTM STP 1427*, L. A. Gritzo and N. J. Alvarez, Eds., American Society for Testing and Materials, West Conshohocken, PA, 2002.
2. Nicolette, V.F. and Hewson, J.C., "Modeling the thermal environment from ambient atmosphere solid propellant fires," JANNAF, Boston, May 2008.
3. Parry, D.L., and Brewster, M.Q., (1991), "Optical Constants of Al2O3 Smoke in Propellant Fires," J. Thermophysics and Heat Transfer, vol. 5, no. 2, pp. 142-149, 1991.
4. Hewson, J.C., Glaze, D.J., and Wagner, G.J., (2008), "A Lagrangian model for evolving particulate flows, sprays, combustion, and its coupling to an Eulerian fluid solver," Sandia National Laboratories report, in preparation.
5. Fuss, S.P., and Hamins, A., (2002), "Determination of Planck Mean Absorption Coefficients for HBr, HCl, and HF," Transactions of the ASME, Vol. 124, p. 26, February 2002.
6. Shah, N.G., "The Computation of Radiation Heat Transfer", Ph.D. thesis, University of London, Dept. of Mechanical Engineering, Imperial College of Science and Technology, London, 1979.